iScience, Volume *23*

Supplemental Information

Disrupting ATF4 Expression Mechanisms Provides an Effective Strategy for BRAF-Targeted Melanoma Therapy

Ikuko Nagasawa, Masaru Koido, Yuri Tani, Satomi Tsukahara, Kazuhiro Kunimasa, and Akihiro Tomida

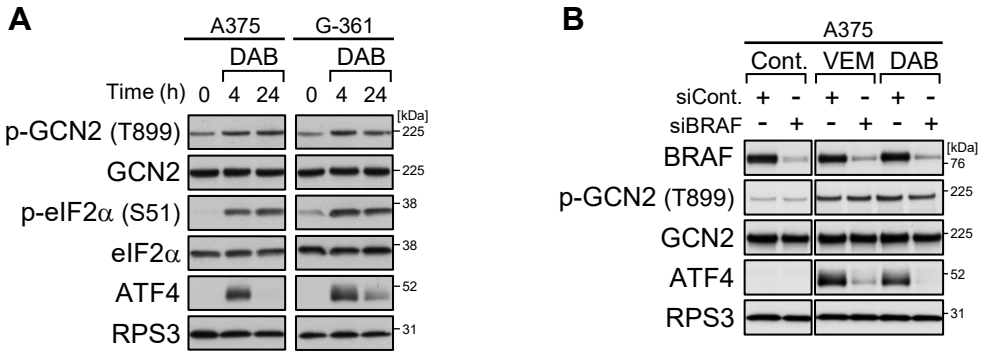

Figure S1. BRAF kinase inhibitors induce ATF4 expression transiently, related to Figure 1.

(**A**) Immunoblot analysis of A375 and G-361 cells treated with dabrafenib (DAB, 1 μM) for 4 or 24 h. (**B**) Immunoblot analysis of A375 and G-361 cells with *BRAF* knockdown by alternative siRNA (Silencer select) and treatment with vemurafenib (VEM, 10 μM) or dabrafenib (1 μM) for 4 h.

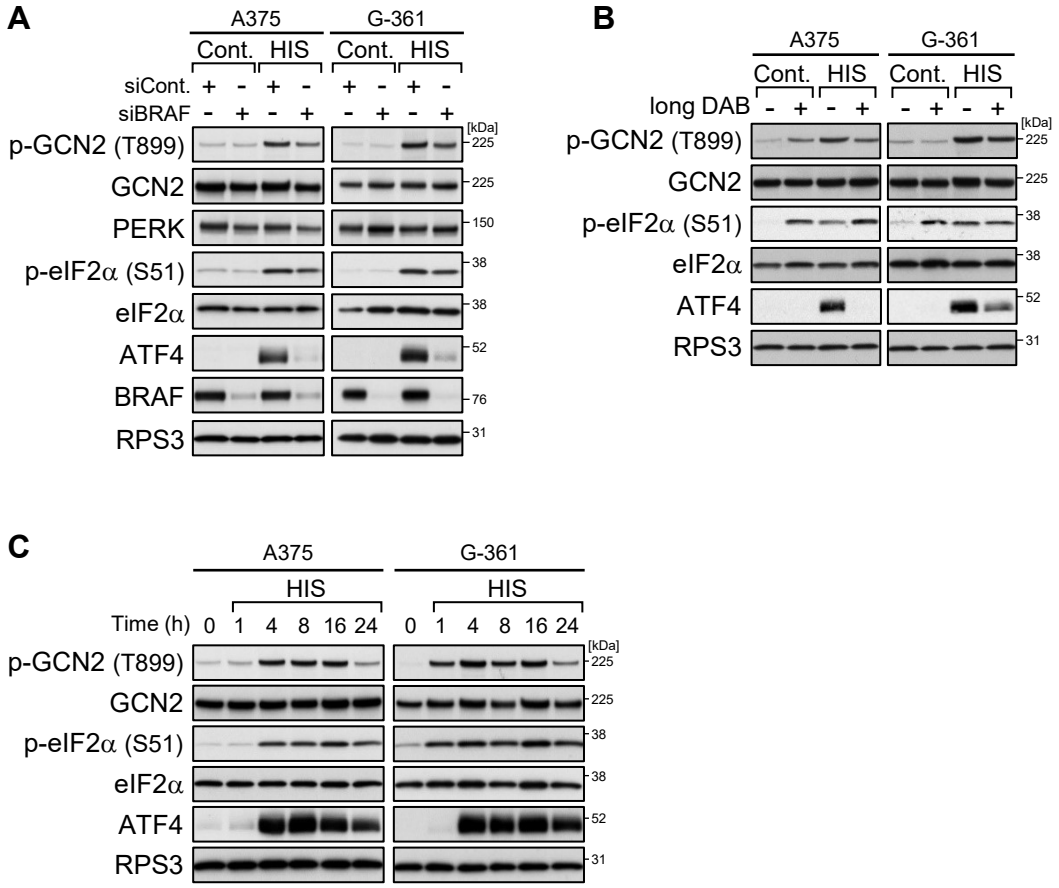

Figure S2. BRAF depletion or prolonged BRAF kinase inhibition prevents ATF4 induction, related to Figure 2.

(**A**) Immunoblot analysis of A375 and G-361 cells with *BRAF* knockdown by alternative siRNA (Silencer select) and treatment with L-histidinol (HIS, 2 mM) for 4 h. (**B**) Immunoblot analysis of A375 and G-361 cells treated with dabrafenib (DAB, 1 μM) for 24 h and then treated with L-histidinol (2 mM) for 4 h. (**C**) Immunoblot analysis of A375 and G-361 cells treated with L-histidinol (2 mM) for the indicated times.

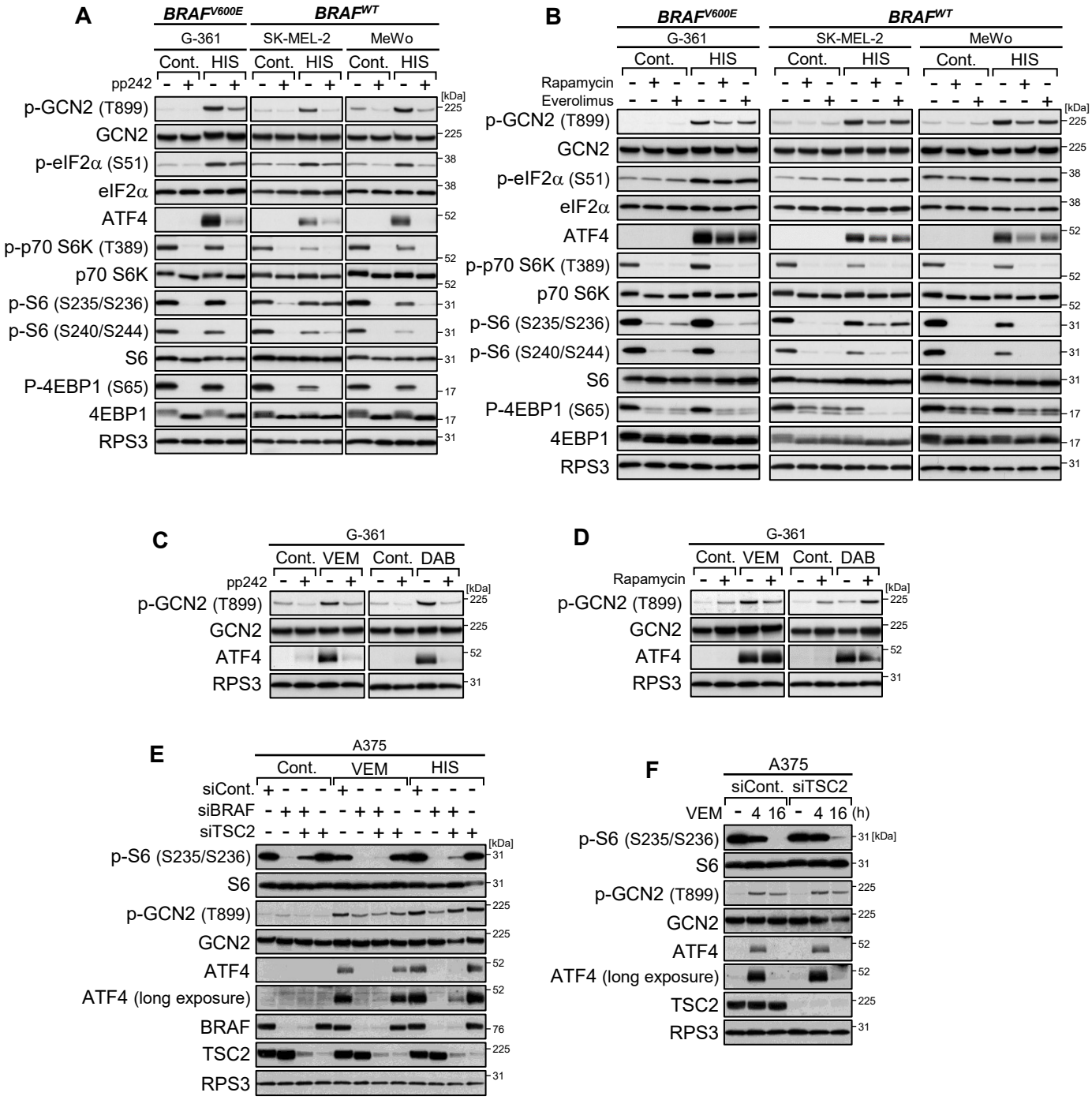

Figure S3. Oncogenic BRAF utilizes mTOR signaling pathway for ATF4 induction, related to Figure 3.

(**A**, **B**) Immunoblot analysis of the melanoma cell lines treated with L-histidinol (HIS, 2 mM) alone or in combination with pp242 (1 μM) (**A**) or with rapamycin (0.1 μM) or everolimus (0.1 μM) (**B**) for 4 h. (**C**, **D**) Immunoblot analysis of G-361 cells treated with vemurafenib (VEM, 10 μM) or dabrafenib (DAB, 1 μM) alone or in combination with pp242 (1 μM) (**C**) or with rapamycin (0.1 μM) (**D**) for 4 h. (**E**, **F**) Immunoblot analysis of A375 cells with *TSC2* knockdown by siRNA (ON-TARGETplus SMARTpool) and treatment with vemurafenib (10 μM) or L-histidinol (2 mM) for 4 h (**E**) or 16 h.

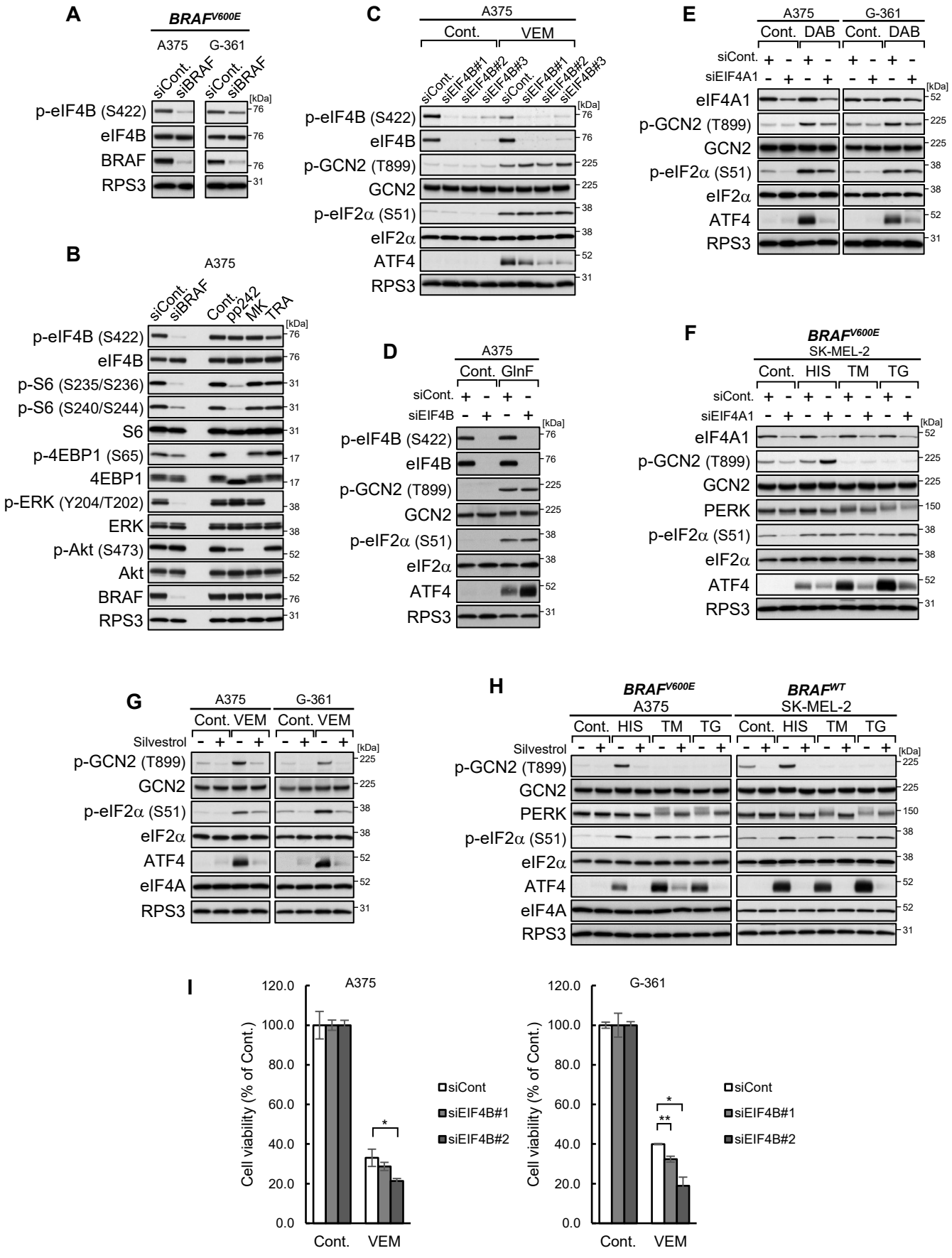
A
BRAFV600E
A375
G-361
siCont.
siBRAF
p-eIF4B (S422)
eIF4B
BRAF
RPS3
[kDa]
B
A375
siCont.
siBRAF
Cont.
pp242
MK
TRA
p-eIF4B (S422)
eIF4B
p-S6 (S235/S236)
p-S6 (S240/S244)
S6
p-4EBP1 (S65)
4EBP1
p-ERK (Y204/T202)
ERK
p-Akt (S473)
Akt
BRAF
RPS3
C
A375
Cont.
VEM
siCont.
siEIF4B#1
siEIF4B#2
siEIF4B#3
p-eIF4B (S422)
eIF4B
p-GCN2 (T899)
GCN2
p-eIF2α (S51)
eIF2α
ATF4
RPS3
D
A375
Cont.
GlnF
siCont.
siEIF4B
p-eIF4B (S422)
eIF4B
p-GCN2 (T899)
GCN2
p-eIF2α (S51)
eIF2α
ATF4
RPS3
E
A375
G-361
Cont.
DAB
siCont.
siEIF4A1
eIF4A1
p-GCN2 (T899)
GCN2
p-eIF2α (S51)
eIF2α
ATF4
RPS3
F
BRAFV600E
SK-MEL-2
Cont.
HIS
TM
TG
siCont.
siEIF4A1
eIF4A1
p-GCN2 (T899)
GCN2
PERK
p-eIF2α (S51)
eIF2α
ATF4
RPS3
G
A375
G-361
Cont.
VEM
Silvestrol
p-GCN2 (T899)
GCN2
p-eIF2α (S51)
eIF2α
ATF4
eIF4A
RPS3
H
BRAFV600E
A375
BRAFWT
SK-MEL-2
Cont.
HIS
TM
TG
Silvestrol
p-GCN2 (T899)
GCN2
PERK
p-eIF2α (S51)
eIF2α
ATF4
eIF4A
RPS3
I
A375
G-361
Cell viability (% of Cont.)
120.0
100.0
80.0
60.0
40.0
20.0
0.0
Cont.
VEM
siCont
siEIF4B#1
siEIF4B#2
*
**

Figure S4. Oncogenic BRAF enhances eIF4B phosphorylation for ATF4 induction, related to Figure 4.

(**A**) Immunoblot analysis of A375 and G-361 cells with *BRAF* knockdown by alternative siRNA (Silencer select). (**B**) Immunoblot analysis of A375 cells with *BRAF* knockdown or treatment with pp242 (1 μM), Akt inhibitor MK-2206 (MK, 1 μM), or trametinib (TRA, 0.1 μM) for 4 h. (**C**) Immunoblot analysis of A375 cells with *EIF4B* knockdown by alternative siRNAs (Silencer select) and treatment with vemurafenib (10 μM) for 4 h. (**D**) Immunoblot analysis of A375 cells with *EIF4B* knockdown cultured in glutamine-free (GlnF) medium for 18 h. (**E**, **F**) Immunoblot analysis of the melanoma cell lines with *EIF4A1* knockdown and treatment with dabrafenib (DAB, 1 μM) (**E**) or with L-histidinol (HIS, 2 mM), tunicamycin (TM, 1 μg/ml), or thapsigargin (TG, 0.3 μM) (**F**) for 4 h. (**G**, **H**) Immunoblot analysis of the melanoma cell lines treated with silvestrol (50 nM) alone or in combination with vemurafenib (10 μM) (**G**) or L-histidinol (2 mM), tunicamycin (1 μg/ml), or thapsigargin (0.3 μM) (**H**) for 4 h. (**I**) A375 and G-361 cells were transfected with *EIF4B*-specific siRNA and treated with vemurafenib (10 μM) for 48 h. Results are shown as the mean ± SD (n=3). The p values were calculated by two-tailed *t*-test. **p < 0.01, *p < 0.05. Results are representative of two independent experiments.

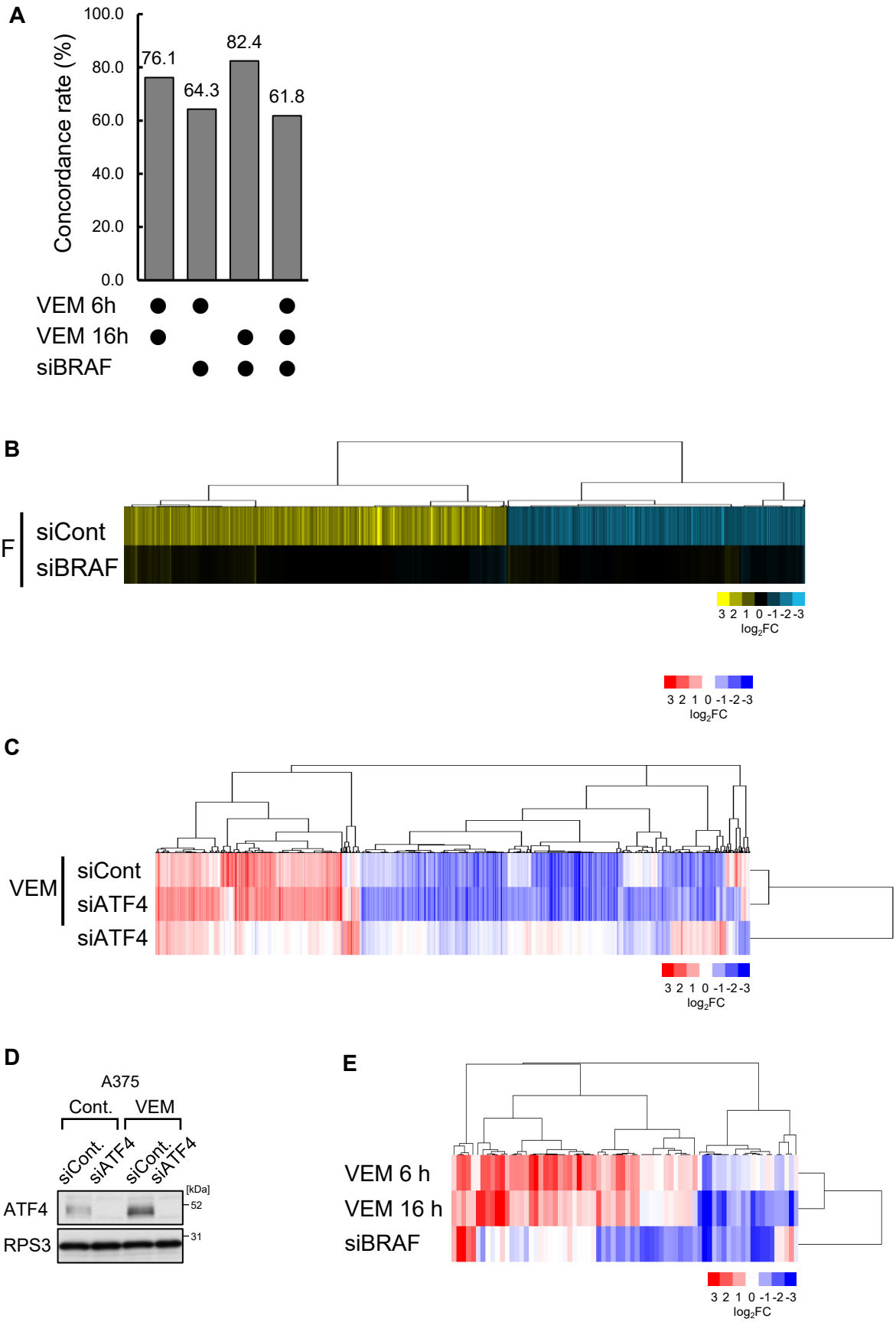
A
Concordance rate (%)
100.0
80.0
60.0
40.0
20.0
0.0
76.1
64.3
82.4
61.8
VEM 6h
VEM 16h
siBRAF
B
GlnF
siCont
siBRAF
3 2 1 0 -1 -2 -3
log2FC
3 2 1 0 -1 -2 -3
log2FC
C
VEM
siCont
siATF4
siATF4
3 2 1 0 -1 -2 -3
log2FC
D
A375
Cont.
VEM
siCont.
siATF4
siCont.
siATF4
[kDa]
ATF4
52
RPS3
31
E
VEM 6 h
VEM 16 h
siBRAF
3 2 1 0 -1 -2 -3
log2FC

Figure S5. Expression of ATF4 target genes is influenced by BRAF inhibition, related to Figure 5.

(**A**) Concordance rates between the BRAF-inhibiting perturbations in Figure 5A. (**B**) Signature of 2,130 probe sets (1,574 genes) that were upregulated or downregulated under glutamine deprivation (GlnF) for 18 h in A375 cells with BRAF knockdown. The log2 fold change of levels upon glutamine deprivation is shown for each indicated knockdown condition. For probe lists, see Table S3. (**C**) Signature of 1,117 probe sets (781 genes) that were either upregulated or downregulated by treatment with vemurafenib and/or knockdown of *ATF4*. A375 cells were transfected with non-targeting siRNA (siCont) or siRNA specific for *ATF4* and then treated with vemurafenib (VEM, 10 μM) for 4 h. The log2 fold change of levels under the indicated conditions is shown for the conditions of transfection with nontargeting siRNA (siCont) and treatment with DMSO. For probe lists, see Supplementary Table S4. (**D**) Immunoblot analysis of A375 cells with *ATF4* knockdown and treatment with vemurafenib (10 μM) for 4 h. (**E**) Signature of 72 probe sets (56 genes) that overlapped between probe sets altered by BRAF-inhibiting perturbations (Figure 5A) and probe sets of the BRAFi**–**ATF4 signature (Figure 5B). For probe lists, see Supplementary Table S6.

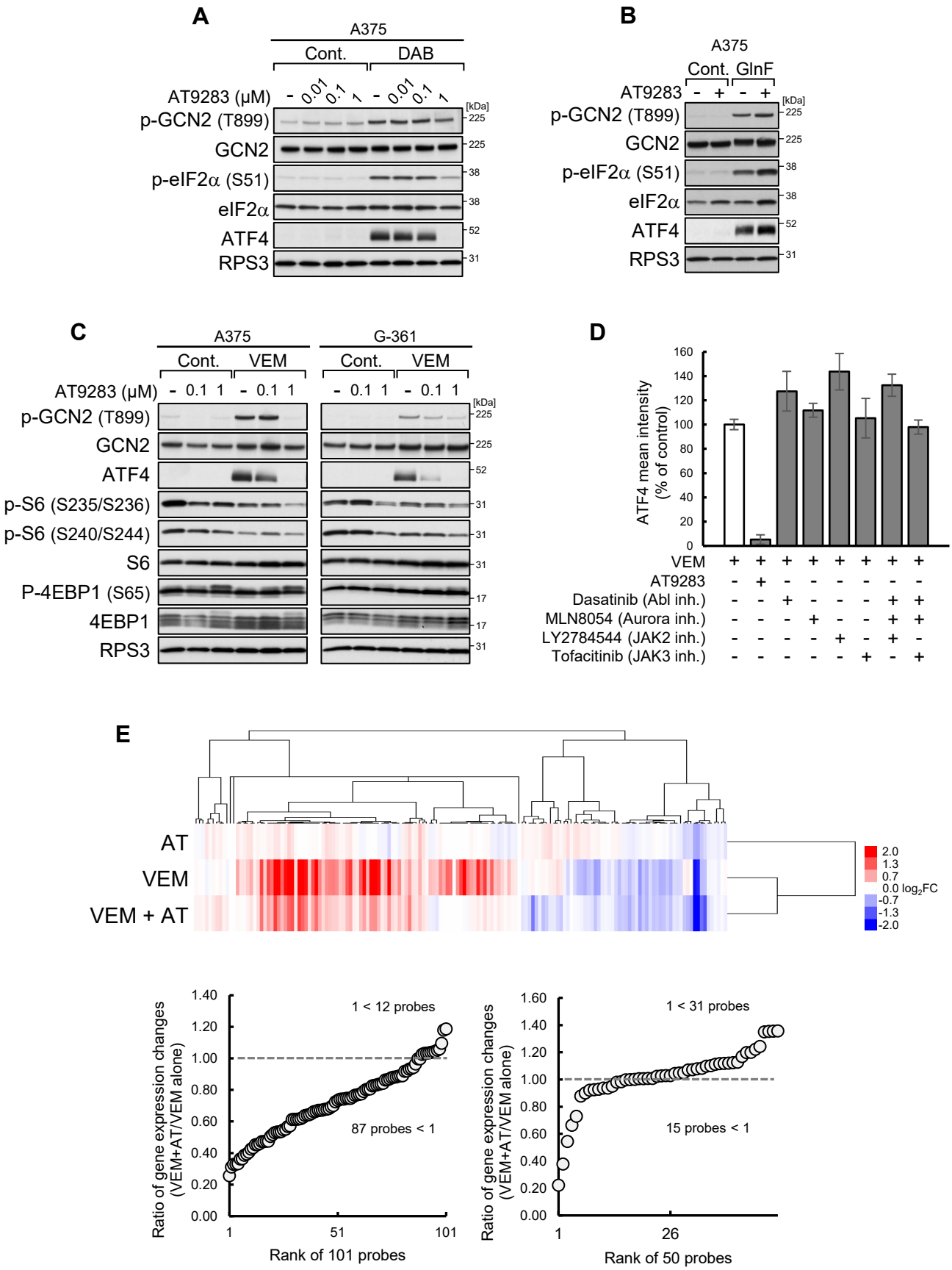
A
A375
Cont.
DAB
AT9283 (μM)
- 0.01 0.1 1 - 0.01 0.1 1
[kDa]
p-GCN2 (T899)
GCN2
p-eIF2α (S51)
eIF2α
ATF4
RPS3
225
225
38
38
52
31
B
A375
Cont. GlnF
AT9283
- + - +
[kDa]
p-GCN2 (T899)
GCN2
p-eIF2α (S51)
eIF2α
ATF4
RPS3
225
225
38
38
52
31
C
A375
G-361
Cont.
VEM
AT9283 (μM)
- 0.1 1 - 0.1 1
[kDa]
p-GCN2 (T899)
GCN2
ATF4
p-S6 (S235/S236)
p-S6 (S240/S244)
S6
P-4EBP1 (S65)
4EBP1
RPS3
225
225
52
31
31
31
17
17
31
D
ATF4 mean intensity
(% of control)
160
140
120
100
80
60
40
20
0
VEM + + + + + + + +
AT9283 - + - - - - - -
Dasatinib (Abl inh.) - - + - - - + +
MLN8054 (Aurora inh.) - - - + - - + +
LY2784544 (JAK2 inh.) - - - - + - + -
Tofacitinib (JAK3 inh.) - - - - - + - +
E
AT
VEM
VEM + AT
2.0
1.3
0.7
0.0 log2FC
-0.7
-1.3
-2.0
Ratio of gene expression changes
(VEM+AT/VEM alone)
1.40
1.20
1.00
0.80
0.60
0.40
0.20
0.00
1 < 12 probes
87 probes < 1
1
51
101
Rank of 101 probes
Ratio of gene expression changes
(VEM+AT/VEM alone)
1.60
1.40
1.20
1.00
0.80
0.60
0.40
0.20
0.00
1 < 31 probes
15 probes < 1
1
26
Rank of 50 probes

Figure S6. Identification of a chemical compound that suppresses GCN2–ATF4 pathway activation during BRAF kinase inhibition, related to Figure 6.

(**A**) Immunoblot analysis of A375 cells treated with AT9283 alone or in combination with dabrafenib (DAB, 1 μM) for 4 h. (**B**) Immunoblot analysis of A375 cells in the presence of AT9283 (1 μM) in glutamine-free (GlnF) medium for 18 h. (**C**) Immunoblot analysis of A375 and G-361 cells treated with AT9283 alone or in combination with vemurafenib (VEM, 10 μM) for 4 h. (**D**) A375 cells were treated with vemurafenib (10 μM) in the presence or absence of AT9283 (1 μM), dasatinib (1 μM), MLN8054 (1 μM), LY2784544 (1 μM), tofacitinib (1 μM), or their combinations for 6 h. The cells were fixed and stained with anti-ATF4 antibody. Bars represent the quantification of the intensity of ATF4 signals in the nucleus. Results are shown as the mean ± SD (n=3). (**E**) Signature of 155 probe sets (BRAFi–ATF4 signature) under the conditions of treatment with vemurafenib (10 μM), AT9283 (0.1 μM), or both for 6 h. The log2 fold change of levels upon treatment with vemurafenib is shown for the condition of treatment with DMSO. Plots represent the ratio of gene expression changes (cotreatment of vemurafenib with AT9283 vs. vemurafenib alone; left panel, rank of 101 probes upregulated by vemurafenib alone; right panel, rank of 50 probes downregulated by vemurafenib alone).

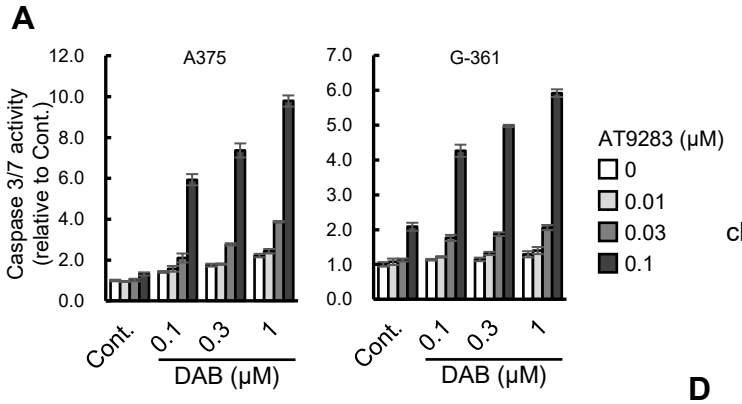
A
A375
G-361
Caspase 3/7 activity (relative to Cont.)
AT9283 (μM)
0
0.01
0.03
0.1
Cont.
DAB (μM)

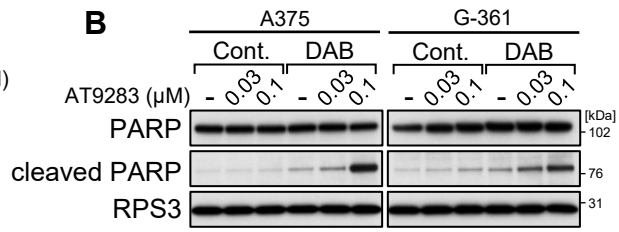
B
A375
G-361
Cont.
DAB
AT9283 (μM)
PARP
cleaved PARP
RPS3
[kDa]
102
76
31

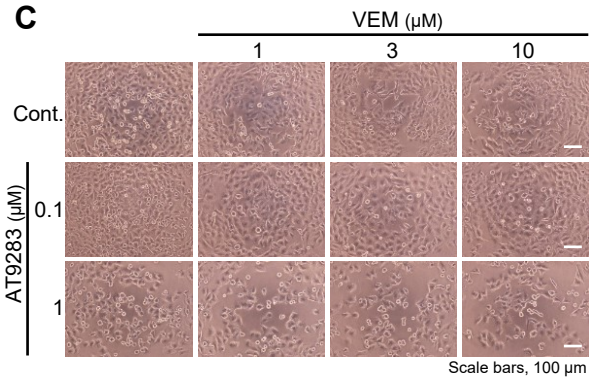
C
VEM (μM)
Cont.
AT9283 (μM)
Scale bars, 100 μm

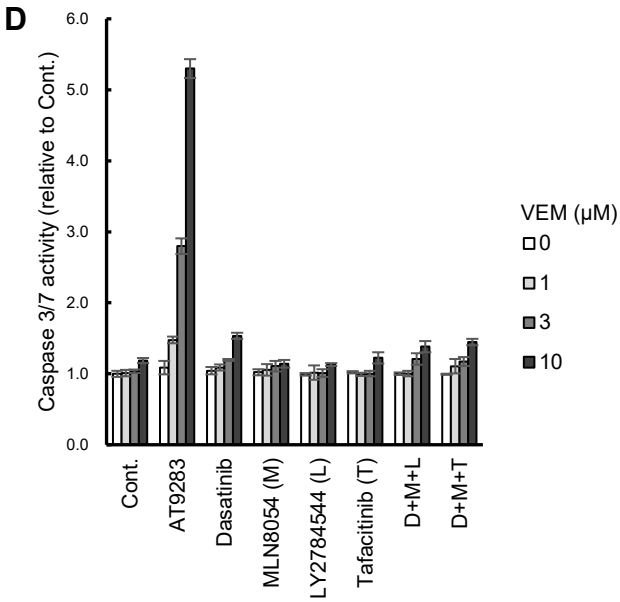
D
Caspase 3/7 activity (relative to Cont.)
VEM (μM)
Cont.
AT9283
Dasatinib
MLN8054 (M)
LY2784544 (L)
Tafacitinib (T)
D+M+L
D+M+T

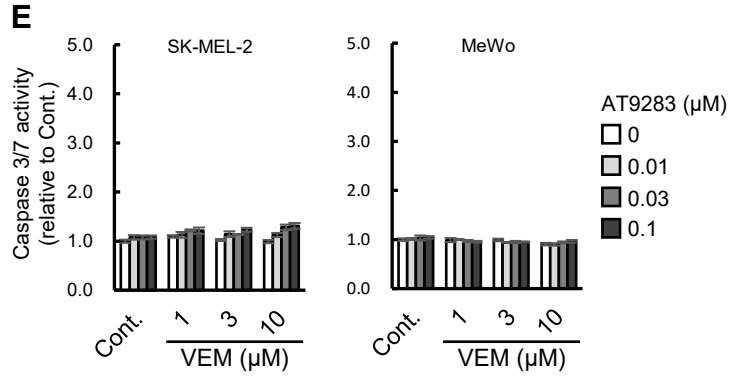
E
SK-MEL-2
MeWo
Caspase 3/7 activity (relative to Cont.)
AT9283 (μM)
VEM (μM)

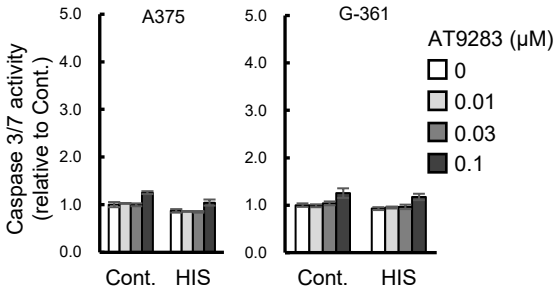
F
A375
G-361
Caspase 3/7 activity (relative to Cont.)
AT9283 (μM)
Cont.
HIS

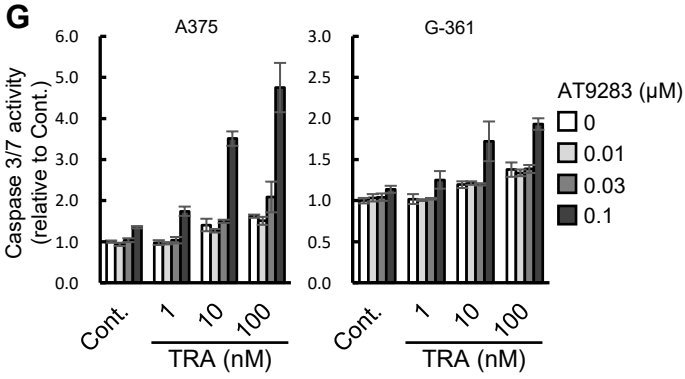
G
A375
G-361
Caspase 3/7 activity (relative to Cont.)
AT9283 (μM)
TRA (nM)

Figure S7. Enhanced growth inhibition by combined treatments with BRAF inhibitors and AT9283, related to Figure 7.

(**A**) A375 and G-361 cells were treated with AT9283 alone or in combination with dabrafenib (DAB) for 16 h. The caspase-3/7 activities were measured by the Caspase-Glo 3/7 assay. Results are shown as the mean ± SD (n=3). (**B**) Immunoblot analysis of A375 and G-361 cells treated with AT9283 alone or in combination with dabrafenib for 16 h. (**C**) Representative images of A375 cells treated with AT9283 alone or in combination with vemurafenib (VEM) for 16 h. (**D**) A375 cells were treated with vemurafenib in the presence or absence of AT9283 (0.1 μM), dasatinib (0.1 μM), MLN8054 (0.1 μM), LY2784544 (0.1 μM), tofacitinib (0.1 μM), or their combinations for 16 h. The caspase-3/7 activities were measured by the Caspase-Glo 3/7 assay. Results are shown as the mean ± SD (n=3). (**E**–**G**) The melanoma cell lines were treated with AT9283 alone or in combination with vemurafenib (**E**), L-histidinol (HIS, 2 mM) (**F**), or trametinib (TRA) (**G**) for 16 h. The caspase-3/7 activities were measured by the Caspase-Glo 3/7 assay. Results are shown as the mean ± SD (n=3).

TRANSPARENT METHODS

Cell lines, Reagents, and Software

Cell lines	Source	Catalog number
A375	ATCC	CRL-1619
G-361	ATCC	CRL-1424
SK-MEL-2	ATCC	HTB-68
MeWo	ATCC	HTB-65
HEK293T	ATCC	CRL-3216

Antibodies	Source	Catalog number
Rabbit monoclonal anti-phospho-eIF2α (Ser51)	Cell Signaling Technology	# 3398
Rabbit monoclonal anti-ATF4	Cell Signaling Technology	# 11815
Rabbit anti-GCN2	Cell Signaling Technology	# 3302
Rabbit monoclonal anti-phospho-p44/42 MAPK (Erk1/2) (Thr202/Tyr204)	Cell Signaling Technology	# 4370
Rabbit monoclonal anti-p44/42 MAPK (Erk1/2)	Cell Signaling Technology	# 4695
Rabbit monoclonal anti-phospho-Akt (Ser473)	Cell Signaling Technology	# 4060
Rabbit monoclonal anti-Akt (pan)	Cell Signaling Technology	# 4685
Rabbit monoclonal anti-phospho-p70 S6 Kinase (Thr389)	Cell Signaling Technology	# 9234
Rabbit anti-p70 S6 Kinase	Cell Signaling Technology	# 9202
Rabbit anti-phospho-S6 Ribosormal Protein (Ser235/236)	Cell Signaling Technology	# 2211
Rabbit anti-phospho-S6 Ribosormal Protein (Ser240/244)	Cell Signaling Technology	# 2215
Rabbit monoclonal anti-S6 Ribosormal Protein	Cell Signaling Technology	# 2217
Rabbit monoclonal anti-TSC2	Cell Signaling Technology	#4308
Rabbit monoclonal anti-phospho-4E-BP1 (Ser65)	Cell Signaling Technology	# 9456

Rabbit monoclonal anti-phospho-4E-BP1	Cell Signaling Technology	# 9644
Rabbit anti-phospho-eIF4B (Ser422)	Cell Signaling Technology	# 3591
Rabbit anti-eIF4B	Cell Signaling Technology	# 3592
Rabbit anti-eIF4A1	Cell Signaling Technology	# 2490
Rabbit monoclonal anti-cleaved PARP (Asp214)	Cell Signaling Technology	# 5625
Rabbit monoclonal anti-PARP	Cell Signaling Technology	# 9532
Rabbit monoclonal anti-phospho-Stat3 (Tyr705)	Cell Signaling Technology	# 9145
Rabbit anti-Stat3	Cell Signaling Technology	# 9132
Rabbit anti-Ribosomal Protein L7a	Cell Signaling Technology	# 2403
Rabbit monoclonal anti-Ribosomal Protein S3	Cell Signaling Technology	# 9538
Rabbit monoclonal anti-phospho-GCN2 (Thr899)	Abcam	ab75836
Rabbit anti-PERK	Abcam	ab65142
Mouse monoclonal anti-EIF2S1	Abcam	ab5369
Mouse monoclonal anti-Raf-B	Santa Cruz Biotechnology	sc-55522
Mouse monoclonal anti-B-Raf (V600E)	NewEast Biosciences	# 26039
Mouse monoclonal anti-FLAG	Sigma-Aldrich	F3165
Goat anti-Rabbit IgG (H+L) Secondary Antibody, Alexa Fluor 488 conjugate	Thermo Fisher Scientific	A-11034

Chemicals	**Source**	**Catalog number**
Vemurafenib	Selleckchem	S1267
Dabrafenib	Selleckchem	S2807
Trametinib	Selleckchem	S2673
AT9283	Selleckchem	S1134
Dasatinib	Selleckchem	S1021
MLN8054	Selleckchem	S1100
LY2784544	Selleckchem	S2179
Tofacitinib	Selleckchem	Kinase Inhibitor Library
MK-2206	Selleckchem	S1078

Kinase Inhibitor Library	Selleckchem	Z88022
PP242	Sigma-Aldrich	N/A
Rapamycin	Sigma-Aldrich	N/A
Everolimus	Sigma-Aldrich	N/A
L-Histidinol dihydrochloride	Sigma-Aldrich	H6647
Thapsigargin	FUJIFILM Wako	205-17283
Tunicamycin	Nacalai Tesque	35638-74
Silvestrol	ChemScene	CS-0543

siRNAs	**Source**	**Catalog number**
ON-TARGETplus SMARTpool BRAF siRNA	Dharmacon	L-003460-00
ON-TARGETplus SMARTpool EIF4B siRNA	Dharmacon	L-020179-00
ON-TARGETplus SMARTpool EIF4A1 siRNA	Dharmacon	L-020178-00
ON-TARGETplus SMARTpool ATF4 siRNA	Dharmacon	L-005125-00
ON-TARGETplus SMARTpool TSC2 siRNA	Dharmacon	L-003029-00
Silencer Select BRAF siRNA	Thermo Fisher Scientific	s2080
Silencer Select EIF4B siRNA #1	Thermo Fisher Scientific	s4573
Silencer Select EIF4B siRNA #2	Thermo Fisher Scientific	s4574
Silencer Select EIF4B siRNA #3	Thermo Fisher Scientific	s4575

Plasmid	**Source**	**Catalog number**
pFLAG-B-Raf	Addgene	40775

Software	**Reference**	
Cluster 3.0	de Hoon et al., 2004	http://bonsai.hgc.jp/~mdehoon/software/cluster/software.htm
DAVID (version 6.8)	Huang da et al., 2009a; Huang da et al., 2009b	https://david.ncifcrf.gov/

Enrichr	Chen et al., 2013; Kuleshov et al., 2016	https://amp.pharm.mssm.edu/Enrichr/
GSEA software (version 2.0.14)	Mootha et al., 2003; Subramanian et al., 2005	http://software.broadinstitute.org/gsea/index.jsp
Java TreeView (version 1.1.6r4)	Saldanha, 2004	http://jtreeview.sourceforge.net/
R (version 3.3.1)	N/A	https://www.r-project.org/
RMAExpress (version 1.0.5)	Irizarry et al., 2003	http://rmaexpress.bmbolstad.com/

Cell culture

The melanoma cell lines and HEK293T cells were maintained in RPMI1640 (FUJIFILM Wako, Osaka, Japan) supplemented with 10% fetal bovine serum and 100 μg/ml kanamycin. For the glutamine withdrawal, cells were cultured in glutamine-free RPMI1640 (FUJIFILM Wako) supplemented with 10% fetal bovine serum and 100 μg/ml kanamycin.

Immunoblot analysis

Immunoblot analysis was performed as described previously (Saito et al., 2009). Briefly, cell lysates were prepared using SDS lysis buffer (62.5 mM Tris-HCl pH6.8, 2% SDS, 10% glycerol, and 50 mM DTT) and protein concentrations were determined using the Bio-Rad protein assay (Bio-Rad, Hercules, CA, USA). Protein samples were subjected to SDS-PAGE and subsequently transferred onto a nitrocellulose membrane. The specific bands were detected using Western Lightning plus ECL (Perkin Elmer, Waltham, MA, USA).

RNA interference

Silencing of human *BRAF*, *TSC2*, *EIF4B*, *EIF4A1*, and *ATF4* expression was performed using ON-TARGETplus SMARTpool siRNA (Dharmacon, Lafayette, CO, USA) or Silencer Select siRNA (Thermo Fisher Scientific, Waltham, MA, USA) with Lipofectamine RNAiMAX (Thermo Fisher Scientific). ON-TARGETplus SMARTpool and Silencer Select siRNAs were used at 20 and 5 nM, respectively. Cells were transfected with each siRNA, in accordance with the manufacturer's reverse-transfection protocol.

Overexpression of BRAF

For BRAF V600E point mutation in the FLAG-BRAF expression vector, site-directed mutagenesis was carried out using a QuickChange Mutagenesis Kit (Agilent Technologies, Santa Clara, CA, USA). Transient transfections into HEK293T and A375 cells were performed using Lipofectamine 2000 (Thermo Fisher Scientific).

Cell viability assay

Cells were transfected with *EIF4B*-specific siRNA and cultured at 1×10^3 (A375) or 2×10^3 (G-361) cells/well in a 96-well plate. After 24 h, the cells were treated with vemurafenib for 48 h. For cell regrowth assay, the cells were seeded at 5×10^3 (A375) or 1×10^4 (G-361) cells/well in a 96-well plate and treated with AT9283, vemurafenib, or both for 16 h. The cells were reseeded to a new 96-well plate and cultured in drug-free medium for 96 h. Cell viability was determined by the CellTiter-Glo luminescent cell viability assay (Promega, Madison, WI, USA) based on quantification of the ATP content.

Chemical screening

A375 cells were seeded at 8×10^3 cells/well in a 96-well plate and treated with each compound (2 μM) from the Kinase Inhibitor Library (355 kinase inhibitors, Selleck) in combination with vemurafenib (10 μM) for 6 h. The cells were fixed and subjected to fluorescent immunostaining using anti-ATF4 antibody as described below.

Fluorescent immunostaining

A375 cells (8×10^3 cells/well in a 96-well plate) were treated with vemurafenib, L-histidinol, or tunicamycin in the presence or absence of kinase inhibitors for 6 h. For comparison of the effects of AT9283, dasatinib, MLN8054, LY2784544, and tofacitinib, cells were treated with each compound at 1 μM, a concentration enough to inhibit each target kinase activity, based on the previous reports (Flanagan et al., 2010; Howard et al., 2009; Ma et al., 2013; Manfredi et al., 2007; O'Hare et al., 2005). The cells were subjected to fluorescent immunostaining using anti-ATF4 antibody, as described previously (Nagasawa et al., 2017). Fluorescent images were acquired by IN Cell Analyzer 6000 (GE Healthcare, Chicago, IL, USA). Quantification of ATF4 intensity in the nucleus was performed using IN Cell Developer Toolbox software (GE Healthcare).

Caspase-3/7 activity assay

Cells were seeded at 5×10^3 (A375) or 1×10^4 (G-361) cells/well in a 96-well plate and treated with vemurafenib, L-histidinol, or trametinib in the presence or absence of AT9283, dasatinib, MLN8054, LY2784544, tofacitinib, or their combinations for 16 h. The caspase-3/7 activities were measured by the Caspase-Glo 3/7 assay (Promega).

Colony formation assay

A375 and G-361 cells were treated with AT9283, vemurafenib, or both for 16 h, and then reseeded in six-well plates (A375: 1×10^3 cells/well, G361: 2×10^3 cells/well). After 7 (A375) or 14 (G-361) days, the colonies were stained with crystal violet.

Microarray

Microarray analysis was carried out as described previously (Saito et al., 2009). The data were normalized by the Robust Multichip Average method using RMAExpress 1.0.5 (Irizarry et al., 2003). Probes with a signal intensity value of < 50 were treated as having a fixed value of 50 (Mashima et al., 2015). Signatures of gene sets were selected using the signal intensity ratio relative to each control sample as follows: probes with fold change > 1.5 (< 0.75) are upregulated (downregulated) ones in Figure 6E; probe with fold change > 2 (< 0.5) are upregulated (downregulated) ones for other signatures. Control samples are described in each figure legend. Clustering analysis was performed using the correlation-based distance and complete linkage method by Cluster 3.0 software (de Hoon et al., 2004) and visualized by Java TreeView (Saldanha, 2004). Gene Ontology analysis was performed using DAVID (National Institute of Allergy and Infectious Diseases, NIH, MD, USA) with the default parameters (Huang da et al., 2009a, b) and Enrichr (Chen et al., 2013; Kuleshov et al., 2016).

TCGA analysis

Preprocessed RNA-sequenced transcriptome data and BRAF mutation status of skin cutaneous melanoma (SKCM; 472 donors), including primary and metastasis tumors, were obtained from The Cancer Genome Atlas (TCGA) (Broad Institute TCGA Genome

Data Analysis Center (2016): Firehose stddata_2016_01_28 run; Broad Institute of MIT and Harvard; doi:10.7908/C11G0KM9) (2015) via the cBioPortal (Cerami et al., 2012; Gao et al., 2013) website (downloaded on 3/26/2017). For log2-scaled expression levels of each gene, we calculated the regression coefficients of BRAF V600* mutation status including V600E, V600G, V600M, V600V, and V600_K601delinsE (166 donors) by regressing out the covariate of NRAS or NF1 mutation status (138 donors), which are mutually exclusive with BRAF mutations. We established rankings of genes in descending order of the fitted coefficients for prerank mode of GSEA analysis with 1×10^4 permutations (Mootha et al., 2003; Subramanian et al., 2005). From the BRAFi–ATF4 signature, we excluded *ATF4* and genes that were not included in the TCGA transcriptome data set and tested the enrichment of the remaining 107 genes. For such processing, we used the statistical computing language R (https://www.r-project.org/; version 3.3.1).

Data and Software Availability

The accession number for the microarray data reported in this paper is National Center for Biotechnology Information Gene Expression Omnibus: GSE136615.

Statistics

Data are presented as mean ± S.D. from at least three independent experiments.

SUPPLEMENTAL REFERENCES

Cerami, E., Gao, J., Dogrusoz, U., Gross, B.E., Sumer, S.O., Aksoy, B.A., Jacobsen, A., Byrne, C.J., Heuer, M.L., Larsson, E.*, et al.* (2012). The cBio cancer genomics portal: an open platform for exploring multidimensional cancer genomics data. Cancer Discov *2*, 401-404.

Chen, E.Y., Tan, C.M., Kou, Y., Duan, Q., Wang, Z., Meirelles, G.V., Clark, N.R., and Ma'ayan, A. (2013). Enrichr: interactive and collaborative HTML5 gene list enrichment analysis tool. BMC bioinformatics *14*, 128.

de Hoon, M.J., Imoto, S., Nolan, J., and Miyano, S. (2004). Open source clustering software. Bioinformatics (Oxford, England) *20*, 1453-1454.

Flanagan, M.E., Blumenkopf, T.A., Brissette, W.H., Brown, M.F., Casavant, J.M., Shang-Poa, C., Doty, J.L., Elliott, E.A., Fisher, M.B., Hines, M.*, et al.* (2010). Discovery of CP-690,550: a potent and selective Janus kinase (JAK) inhibitor for the treatment of autoimmune diseases and organ transplant rejection. Journal of medicinal chemistry *53*, 8468-8484.

Gao, J., Aksoy, B.A., Dogrusoz, U., Dresdner, G., Gross, B., Sumer, S.O., Sun, Y., Jacobsen, A., Sinha, R., Larsson, E.*, et al.* (2013). Integrative analysis of complex cancer genomics and clinical profiles using the cBioPortal. Science signaling *6*, pl1.

Huang da, W., Sherman, B.T., and Lempicki, R.A. (2009a). Bioinformatics enrichment tools: paths toward the comprehensive functional analysis of large gene lists. Nucleic acids research *37*, 1-13.

Huang da, W., Sherman, B.T., and Lempicki, R.A. (2009b). Systematic and integrative analysis of large gene lists using DAVID bioinformatics resources. Nature protocols *4*, 44-57.

Irizarry, R.A., Hobbs, B., Collin, F., Beazer-Barclay, Y.D., Antonellis, K.J., Scherf, U., and Speed, T.P. (2003). Exploration, normalization, and summaries of high density oligonucleotide array probe level data. Biostatistics (Oxford, England) *4*, 249-264.

Kuleshov, M.V., Jones, M.R., Rouillard, A.D., Fernandez, N.F., Duan, Q., Wang, Z., Koplev, S., Jenkins, S.L., Jagodnik, K.M., Lachmann, A.*, et al.* (2016). Enrichr: a comprehensive gene set enrichment analysis web server 2016 update. Nucleic acids research *44*, W90-97.

Ma, L., Clayton, J.R., Walgren, R.A., Zhao, B., Evans, R.J., Smith, M.C., Heinz-Taheny, K.M., Kreklau, E.L., Bloem, L., Pitou, C.*, et al.* (2013). Discovery and characterization of LY2784544, a small-molecule tyrosine kinase inhibitor of JAK2V617F. Blood cancer journal *3*, e109.

Manfredi, M.G., Ecsedy, J.A., Meetze, K.A., Balani, S.K., Burenkova, O., Chen, W.,

Galvin, K.M., Hoar, K.M., Huck, J.J., LeRoy, P.J.*, et al.* (2007). Antitumor activity of MLN8054, an orally active small-molecule inhibitor of Aurora A kinase. Proceedings of the National Academy of Sciences of the United States of America *104*, 4106-4111.

Mashima, T., Ushijima, M., Matsuura, M., Tsukahara, S., Kunimasa, K., Furuno, A., Saito, S., Kitamura, M., Soma-Nagae, T., Seimiya, H.*, et al.* (2015). Comprehensive transcriptomic analysis of molecularly targeted drugs in cancer for target pathway evaluation. Cancer science *106*, 909-920.

Mootha, V.K., Lindgren, C.M., Eriksson, K.F., Subramanian, A., Sihag, S., Lehar, J., Puigserver, P., Carlsson, E., Ridderstrale, M., Laurila, E.*, et al.* (2003). PGC-1alpha-responsive genes involved in oxidative phosphorylation are coordinately downregulated in human diabetes. Nature genetics *34*, 267-273.

O'Hare, T., Walters, D.K., Stoffregen, E.P., Jia, T., Manley, P.W., Mestan, J., Cowan-Jacob, S.W., Lee, F.Y., Heinrich, M.C., Deininger, M.W.*, et al.* (2005). In vitro activity of Bcr-Abl inhibitors AMN107 and BMS-354825 against clinically relevant imatinib-resistant Abl kinase domain mutants. Cancer research *65*, 4500-4505.

Saito, S., Furuno, A., Sakurai, J., Sakamoto, A., Park, H.R., Shin-Ya, K., Tsuruo, T., and Tomida, A. (2009). Chemical genomics identifies the unfolded protein response as a target for selective cancer cell killing during glucose deprivation. Cancer research *69*, 4225-4234.

Saldanha, A.J. (2004). Java Treeview--extensible visualization of microarray data. Bioinformatics (Oxford, England) *20*, 3246-3248.

Subramanian, A., Tamayo, P., Mootha, V.K., Mukherjee, S., Ebert, B.L., Gillette, M.A., Paulovich, A., Pomeroy, S.L., Golub, T.R., Lander, E.S.*, et al.* (2005). Gene set enrichment analysis: a knowledge-based approach for interpreting genome-wide expression profiles. Proceedings of the National Academy of Sciences of the United States of America *102*, 15545-15550.